Tree Physiology 32, 49–64
doi:10.1093/treephys/tpr134

Research paper

High-frequency analysis of the complex linkage between soil CO_2 fluxes, photosynthesis and environmental variables

Jonathan G. Martin[1,4], Claire L. Phillips[2], Andres Schmidt[1], James Irvine[3] and Beverly E. Law[1]

[1]Oregon State University, Department of Forest Ecosystems and Society, 321 Richardson Hall, Corvallis, OR 97331, USA; [2]Center for Accelerator Mass Spectrometry, Lawrence Livermore National Laboratory, P.O. Box 808, L-397, Livermore, CA 94551, USA; [3]Yellowstone Ecological Research Center, 2048 Analysis Dr., Bozeman, MT 59718, USA; [4]Coresponding author (jonathan.martin@oregonstate.edu)

Received May 25, 2011; accepted November 24, 2011; published online January 6, 2012; handling Editor Michael Ryan

High-frequency soil CO_2 flux data are valuable for providing new insights into the processes of soil CO_2 production. A record of hourly soil CO_2 fluxes from a semi-arid ponderosa pine stand was spatially and temporally deconstructed in attempts to determine if variation could be explained by logical drivers using (i) CO_2 production depths, (ii) relationships and lags between fluxes and soil temperatures, or (iii) the role of canopy assimilation in soil CO_2 flux variation. Relationships between temperature and soil fluxes were difficult to establish at the hourly scale because diel cycles of soil fluxes varied seasonally, with the peak of flux rates occurring later in the day as soil water content decreased. Using a simple heat transport/gas diffusion model to estimate the time and depth of CO_2 flux production, we determined that the variation in diel soil CO_2 flux patterns could not be explained by changes in diffusion rates or production from deeper soil profiles. We tested for the effect of gross ecosystem productivity (GEP) by minimizing soil flux covariance with temperature and moisture using only data from discrete bins of environmental conditions (±1 °C soil temperature at multiple depths, precipitation-free periods and stable soil moisture). Gross ecosystem productivity was identified as a possible driver of variability at the hourly scale during the growing season, with multiple lags between ~5, 15 and 23 days. Additionally, the chamber-specific lags between GEP and soil CO_2 fluxes appeared to relate to combined path length for carbon flow (top of tree to chamber center). In this sparse and heterogeneous forested system, the potential link between CO_2 assimilation and soil CO_2 flux may be quite variable both temporally and spatially. For model applications, it is important to note that soil CO_2 fluxes are influenced by many biophysical factors, which may confound or obscure relationships with logical environmental drivers and act at multiple temporal and spatial scales; therefore, caution is needed when attributing soil CO_2 fluxes to covariates like temperature, moisture and GEP.

Keywords: belowground carbon allocation, gross ecosystem productivity, photosynthesis, soil CO_2 efflux, soil respiration.

Introduction

Belowground biological and physical processes play an important role in the global carbon cycle through the regulation of soil carbon. However, these processes can be quite variable due to direct and indirect effects of climate, production and disturbance. Furthermore, soil CO_2 production from organic matter decomposition and respiration from roots and the associated rhizosphere have separate responses to environmental drivers that can be modulated by substrate availability (Pendall et al. 2004), which makes soil carbon processes difficult to quantify. Although soil CO_2 fluxes have long been identified as the largest natural source of C to the atmosphere in most undisturbed and unmanaged terrestrial systems (Schlesinger 1977) and the largest component of terrestrial ecosystem respiration (Law et al. 1999, Janssens et al. 2001, Bolstad et al. 2004), soil CO_2 production and transport are still poorly understood.

A large body of work has focused on simple correlations between temperature and/or moisture and soil surface CO_2

efflux, produced from decomposition and autotrophic respiration. This has been somewhat limited by data availability, which hinders understanding these mechanisms for improving process models (Ryan and Law 2005). Because soil CO_2 fluxes appear to be driven largely by temperature through decomposition (Lloyd and Taylor 1994), soil CO_2 fluxes have been implicated as a potential positive feedback to global temperature increases (Raich and Schlesinger 1992). Recent studies have extrapolated from these general trends at large spatial and temporal scales (Bond-Lamberty and Thomson 2010), but work at smaller scales has highlighted inconsistencies in simple temperature correlations (Kuzyakov and Gavrichkova 2010, Subke and Bahn 2010) and may change some of the global-scale conclusions.

At many research locations, deployments of continuous automated soil CO_2 measurement systems have replaced periodic point measurements. It was hoped that seasonal time courses could be quantified instead of being estimated from linear filling methods or empirical models, which has been the standard for many years (as used in Martin and Bolstad 2009). However, through the use of automated datasets of high-frequency soil CO_2 fluxes, unique properties of soil fluxes have been observed. Some of these include (i) diel hysteresis between the flux and soil temperature (Riveros-Iregui et al. 2007), (ii) seasonal changes in apparent temperature sensitivity (Ruehr and Buchmann 2010), and (iii) correlations between aboveground process and soil CO_2 fluxes (Vargas et al. 2011). These properties have led to theories about detecting links between soil CO_2 fluxes and phenology, photosynthesis, or other daily, seasonal or annual variation of aboveground activity. If a quantifiable link between these processes can be found, the accuracy of carbon models will increase greatly because many currently use simple representations of soil carbon processes (Heimann and Reichstein 2008, Sitch et al. 2008, Chapin et al. 2009, Sierra et al. 2010), and the representation of respiration is a primary cause for uncertainties (Mitchell et al. 2011).

Isotopic tracer studies have shown a direct link between CO_2 respired from the soil surface and recently fixed C from canopy photosynthate production (Horwath et al. 1994, Andrews et al. 1999, Kuzyakov and Cheng 2001), although the contribution to the total soil flux was small. Other attempts to indirectly link carbon assimilation to soil CO_2 fluxes have resulted in similar trends. Manipulation studies have shown that changing gross ecosystem productivity (GEP) through shading (Bahn et al. 2008), girdling (Högberg et al. 2009, Subke et al. 2010) or selective watering (Irvine et al. 2005) directly influences soil fluxes. These impacts are assumed to be from direct controls on GEP and not changes in other conditions such as temperature, moisture, etc. While some of these patterns may be real (Carbone et al. 2008), others may arise due to false assumptions or spurious correlations. Many of the reported relationships between soil fluxes and aboveground conditions could be artifacts of co-varying data and the inability to separate concurrent diel trends of radiation, temperature, canopy activity and/or wind speed (and hence atmospheric CO_2 gradients), which all share a 24-h cycle.

Adding to this complexity and the errors of assigning causality in the GEP–soil flux pathway could be the erroneous conclusions arising from an unintended spatial mismatch between a flux and a soil temperature from too shallow or too deep a depth (Maljanen et al. 2002, Graf et al. 2008, Phillips et al. 2010), or from a temporal mismatch caused by soil diffusive properties or by the buffered pathway between assimilated and respired C (Subke et al. 2010). Because of the complexity of understanding hourly soil CO_2 fluxes, the question becomes, how to best examine these processes to determine if real quantifiable links between soil CO_2 fluxes, soil climate and canopy assimilation can be made? To address this question, we:

(i) Illustrate that two scenarios, represented by changing either diffusion properties or CO_2 production depths, do not explain diel patterns of hourly soil CO_2 fluxes when common assumptions are utilized (Figure 1).
(ii) Explore a third scenario where the source of CO_2 becomes dominated by recent photosynthesis and creates the seasonal shifts in diel timing of soil fluxes. This is accomplished through unbiased data bins that remove temperature and moisture effects (Figure 1).
(iii) Propose that the spatial relationships between canopy assimilation soil fluxes may be chamber specific when compared against vegetation survey data.

Methods

Site location and description

This study presents data from a mature (aged 66 years) ponderosa pine (*Pinus ponderosa* Doug. Ex P. Laws) forest in the

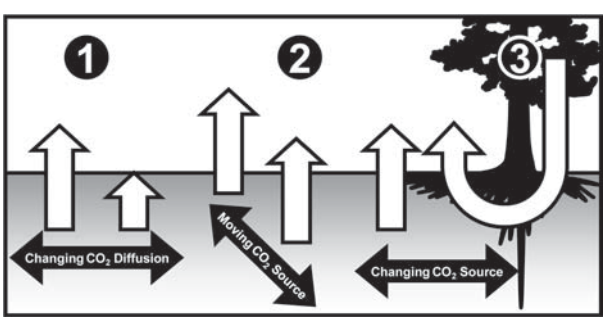

Figure 1. Three possible scenarios that may influence the seasonality of diel patterns of soil CO_2 fluxes. Scenario 1: changes in diffusion coefficients between wet and dry periods could influence the rate of CO_2 transport from sites of production to surface measurement locations. Scenario 2: the dominant source of soil CO_2 production may migrate to deeper soil layers as upper layers dry. Scenario 3: the dominant C source of CO_2 may change seasonally from decomposition of soil substrate to photosynthate or photosynthate-primed microbial activity.

Deschutes National Forest, OR, USA (44.452 N, 121.557 W, 1253 m), and is part of the AmeriFlux network of eddy flux covariance sites (http://public.ornl.gov/ameriflux/, AmeriFlux site code: USME-2; site descriptions, detailed site data, locations and histories are available online). The site is semi-arid (1982–2007 mean annual precipitation was 535 mm) and temperate (minimum, mean and maximum annual temperature: 14.2, 7.5 and 32.9 °C for 2002–2008), with sandy-textured andisols (Thomas et al. 2009). The site was harvested in ~1915 and allowed to regenerate naturally. The canopy is dominated by ponderosa pine (*P. ponderosa*) and incense cedar (*Calocedrus decurrens* (Torr.) Florin) with an average canopy height of 16.6 m, a mean diameter of 30 cm, a density of 325 trees ha^{-1} and a leaf area index (LAI) of 2.8. The understory is composed of bitterbrush (*Purshia tridentata* (Push) DC.) and manzanita (*Arctostaphylos patula* Greene) with an LAI of 0.2. Site survey data were available from existing work (Irvine et al. 2008).

Measuring soil respiration and soil climate

Soil respiration was measured with a LI-COR 8100 fitted with an 8150 multiplexer unit (LI-COR Biosciences, Lincoln, NE, USA) located within 100 m of the eddy flux tower. We used four chambers: C1 was 0.6 m from a mature ponderosa pine tree, C2 and C3 were interspersed in bitterbrush and trees and were 1.2 and 1.8 m from the base of the nearest tree, respectively, and C4 was isolated from trees (3.4 m from the base of the nearest tree) in a bitterbrush clearing. Based on the stand survey data, we calculated that the average midpoint distance between individual trees was 3.13 m; therefore, our chamber deployment layout represents a similar range of distances from individual trees experienced at this site (Figure 2).

Soil respiration was logged hourly, after a 3-min measurement cycle per chamber that included a 30-s dead band and a 30-s purge between chambers. Data were filtered for anomalous or erroneous values caused by mechanical faults such as a poor chamber seal, flow problems or damaged instrumentation, resulting in 39% data coverage for a 1.5-year period. Most missing data periods were in cohesive blocks, and were due to power loss or severe winter conditions.

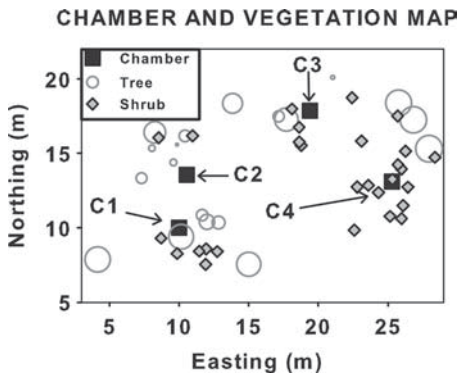

Figure 2. A map of chamber location and vegetation position/composition showing the range of proximity and types of vegetation relative to chamber position. Tree symbol diameter is scaled to tree diameter at breast height (1.37 m). Path lengths are the combined distance of tree height and distance from tree base to chamber.

Soil meteorological data were collected using standard AmeriFlux guidelines (http://public.ornl.gov/ameriflux/). Soil temperature was measured using thermocouples at 2, 3, 8, 16, 32 and 64 cm depths with 10 replicates at 2, 4, 6 and 16 cm. Spatial variation was minimal at the shallow depths, so deeper variation was assumed to be minimal. Volumetric soil moisture was measured at 10, 20, 30, 50, 70, 100, 130 and 160 cm depths using three Envirosmart probes (Sentek Sensor Technologies, Stepney, SA, Australia). Data were logged every 30 min using a Campbell Scientific 10× logger (Campbell Scientific Inc., Logan, UT, USA).

Gross ecosystem exchange of CO_2 (GEP) was estimated from eddy-covariance measurements that were collected using a 3D sonic anemometer (model CSAT3, Campbell Scientific Inc.) and an open-path infrared gas analyzer (model LI-7500, LI-COR Inc., Lincoln, NE, USA) at 33 m above ground level (see Thomas et al. (2009) and Vickers et al. (2012) for complete site descriptions, instrument usage and data processing).

Estimating diffusion parameters

Understanding the hourly and diel patterns of soil CO_2 flux require estimates of soil CO_2 production and transport. We did not have buried CO_2 sensors to capture the timing of production; however, we were able to estimate the depth of production using the thermal transfer and diffusion properties of soil. Soil thermal transfer, not CO_2 diffusivity, has been identified as the main driver of lags between soil production at different layers (Phillips et al. 2010), so we believe that the lags between production and measurements at the surface will be largely driven by the inherent lags in soil temperatures at different depths; however, CO_2 diffusivity should be accounted for as well. Diffusion coefficients were calculated on an hourly basis using soil temperature, soil moisture and soil texture data following the diffusion equations of Rolston and Moldrup (2002), Moldrup et al. (2003) and Riveros-Iregui et al. (2008):

$$D_s = D_{a0}\left(\frac{T}{T_0}\right)^{1.75}\left(\frac{P_0}{P}\right)\times\Phi^2\left(\frac{\varepsilon}{\Phi}\right)^{2+(3/(13.6\times CF+3.5))} \quad (1)$$

D_s is the diffusivity of soil; D_{a0} is the standard diffusivity of CO_2 in air (1.47×10^{-5} m^2 s^{-1}) adjusted by temperature and pressure fluctuations relative to standard temperature (T_0) and pressure (P_0). To compute porosity (Φ), we used homogenized site-specific profile means from 0 to 20 cm soil samples for clay fraction (CF) = 0.07, bulk density (B_D) = 1.14 g cm^{-3}, organic matter fraction (OM_f) = 0.019, organic matter density (OM_D) = 1.4 g cm^{-3}, mineral particle density (MP_D) = 2.7 g cm^{-3}

and air filled pore space (ε) = 1 – volumetric water content (θ). Porosity (Φ) can be calculated as

$$\Phi = \frac{B_D}{((OM_F \times OM_D) + (1 - OM_F) \times MP_D)} \quad (2)$$

In addition to measuring the diffusion coefficients for each hour, we computed the approximate path length time of diffusion using the equation (Heitjans and Kärger 2005)

$$L_d = \sqrt{(4D_s t)} \quad (3)$$

where L_d is the one-dimensional path length in meters, D_s is the diffusion coefficient calculated above using Eq. (1) and t is the time in seconds to travel distance L_d in meters. Equation (3) can be rearranged to solve for t:

$$t = \frac{L_d^2}{4D_s} \quad (4)$$

Equation (4) was used to calculate the path length time for diffusion to occur at soil depth L_d, where L_d is 2, 4, 8, 16, 32 and 64 cm. This time (t) was then added to the observed hour of the peak diel temperature at each depth, which provided an estimate of the hour of day a flux would occur if produced at depth = L_d. These daily values were then regressed against the depth of production to produce a predictive model of the depth of production where the independent variable was the hour of day (Eq. (5)). Also, to account for changes in thermal diffusivity with varying soil moisture, soil moisture was included in the model, which took the form of

$$L_d = -21.026 - 42.743(SWC) + 124.915(SWC^2) + 2.416(H) - 0.012(H^2) - 0.325(SWC \times H) \quad (5)$$

H is equal to the hour of day when the peak diel flux occurred, SWC is the volumetric soil water content ($m^3\ m^{-3}$) and the term SWC × H is an interaction between volumetric soil water and the hour of day. All numerical terms in the model represent estimated parameters and were significant with P values <0.0001 and $r^2 = 0.88$ (all subsequent analysis was performed with JMP 8, SAS Institute Inc., Cary, NC, USA). This empirical model is primarily driven by the observed lags of soil temperature at various depths relative to surface temperatures. If estimates of D_s or L_d are biased, the errors will be small compared with the effect of thermal lags on soil CO_2 production (Phillips et al. 2010). Lastly, this model is site-specific and purely empirical; therefore, additional work should consider alternative methods of modeling soil heat transfer across multiple sites (see Bond-Lamberty et al. 2005).

Testing Scenario 1: changing diffusion properties

The peak values of soil CO_2 flux for each chamber were determined for each day where data acquisition was >50%. We used the simple thermal transport model paired with the diffusion depth model (Eq. (5)) to estimate the depth at which a surface CO_2 flux measurement was produced. This modeling exercise was used to provide two useful estimates: (i) the hour that a flux from a given depth would diffuse from the soil surface and (ii) the depth of a soil flux given that the soil flux would correspond to a specific diel thermal pattern. This technique requires many assumptions: foremost is that a 'pulse' or peak of diel temperature for the day would correspond with instantaneous peak rate of soil CO_2 production at depth. In addition to the flux being thermally driven, we must assume that it occurs at a discrete and finite location, and only diffuses upward and not laterally. The assumption of temperature solely driving the flux is the most contentious, and will be discussed in the following sections where it will be tested. The assumption of flux production at discrete locations is also problematic because integrated fluxes are produced in the profile, from the uppermost layer of recent litter down to the deepest root, and not just at a single point. However, this assumption works very conservatively for our analyses because we are essentially modeling the production at the lowest possible depth given the observed conditions. If the assumption was false and the flux was produced at a more shallow depth, the lags between the flux and temperatures at the depth would be even greater.

Testing Scenario 2: testing temperature responses at depth

Much work has focused on determining the rate of soil CO_2 flux production in relation to soil temperatures, but usually only at a single fixed depth. Here we compared theoretical temperature responses provided the assumptions used in previous analyses were true. We used the predicted depth of the flux evolution to predict temperature responses using standard Q_{10} methods (Fang and Moncrieff 2001). Data from midsummer, where predicted depth was greatest, were used to calculate Q_{10} responses at 32 cm depth. This depth best corresponded to the lower limit of flux production and happened to coincide with available temperature data depth. Daily minimum and maximum values of soil CO_2 flux were paired with minimum and maximum values of 32 cm soil temperature. Each was averaged over a weekly period and Q_{10} values were approximated using

$$Q_{10} = \left(\frac{R_2}{R_1}\right)^{10/(T_2 - T_1)} \quad (6)$$

where R_2 and R_1 are respiration rates at temperatures T_2 and T_1. This method assumes total temperature dependence; there is a large amount of literature from incubation studies that supports the role of temperature in soil CO_2 fluxes (Fang and Moncrieff 2001, Gabriel and Kellman 2011), and our analysis

only examines small temporal periods where soil moisture variation would not influence the flux.

To examine the efficacy of an annual model for predicting hourly fluxes, a soil CO_2 flux model was created using a log-transformed polynomial function with soil moisture and soil temperature from different depths (Martin and Bolstad 2005).

$$\log(\text{Flux}) = a - b(T_d) + c\left(\frac{1}{\text{SWC}}\right) + d\left(\frac{1}{\text{SWC}}\right)^2 + e\left(T_d \times \frac{1}{\text{SWC}}\right) + f(\text{YEAR}) \quad (7)$$

The model uses hourly soil flux (Flux, μmol CO_2 m^{-1} s^{-1}), soil temperature at one of either of three depths (2, 16 or 32 cm; T_d in °C) and the reciprocal of profile integrated soil moisture (SWC, %).

Testing Scenario 3: developing bias-free soil CO_2 flux GEP correlations

To address the issue of potential controls of canopy processes on soil CO_2 fluxes, we used a bias-minimizing binning of the data to ensure that temperature and moisture influences were small or even non-existent. Temperature, moisture and precipitation have been widely cited as driving temporal variation of soil CO_2 fluxes (Fang and Moncrieff 2001, Martin and Bolstad 2005, Ruehr et al. 2010). Including any variation of these factors when testing for correlation of other factors that co-vary could influence the relationships and underlying conclusions. Temperature could be the predominant driver of soil CO_2 fluxes at the daily scale and it co-varies with GEP; therefore, potential temperature effects need to be removed through normalization procedures that do not rely on assumption-driven modeling. We used bins that consisted of (i) precipitation-free periods where there was no measurable precipitation for the previous 5 days, (ii) periods of seasonally consistent soil water content represented by profile integrated soil moisture for 0–1.6 m, which was calculated as a mean of soil moisture weighted by vertical distance between sensors, and (iii) ±1 °C in two separate soil temperature depths, 2 and 16 cm. Two bins of temperatures from shallow and moderate depths were required because single temperature bins resulted in considerable variation at the other measurement depths. Using two depth bins reduced this variation to ~± 1 °C for all soil temperature measurement depths (2–64 cm).

Chamber-specific soil CO_2 flux data from these bins were compared to the 6-h running mean of GEP using a cross-correlation analysis to determine Spearman correlation coefficients at hourly lags from 0 to 30 days (0–720 h). The 6-h running mean of GEP was chosen because it integrates multiple hours of GEP data which can be very noisy at the hourly scale, and because GEP is likely to interact with soil processes at longer time scales. The 6-h running mean of GEP was calculated from the 3-h preceding and following a given hour to ensure temporal patterns were similar to raw GEP data. Cross-correlation results were filtered by significance level (P values >0.05 only) for non-zero slopes (slope >± 0.001), for isolated spikes (significant correlations must be longer than two consecutive hours) and for stationarity (correlations must be 50% greater than the mean value). Filtering for small or near-zero slopes eliminates significant correlations that have no logical relationship, and short-duration peaks are not supported by the work of others that show the carbon pathway from foliage to rhizosphere to be smeared over multiple hours and days even in grasses and small trees (De Deyn et al. 2011, Epron et al. 2011). Stationarity is indicative of no real lagged relationship over the time series regardless of significance or correlation strength.

To further increase the robustness of the cross-correlation analysis, we repeated the exercise across spring (May/June), summer (July/August) and fall (September/October) with two separate sets of binning conditions for each time period. All sets of binned conditions represented the precipitation-free periods with consistent soil moisture and the greatest number of available data from the two bins of temperature data (Table 1). The data during the selected bins are from consistently wet or uniformly dry summer/autumn conditions, and each bin spans fairly short periods of ~20–40 days beginning between Days 128 and 293 (see Table 1 for a complete description of conditions). The summer bins do coincide with seasonally large root contribution to total soil respiration for this site (as shown in Irvine et al. (2008) for the period immediately following trench establishment).

Results and discussion

General patterns of soil climate and soil CO_2 fluxes

Soil CO_2 fluxes from the four chambers had similar seasonal patterns that varied typically with soil temperature and soil moisture, yet the spatial variation among all chambers was high (Figure 3a). Chamber 1 had noticeably the highest flux with maximum values >12 μmol CO_2 m^2 s^{-1}. These values are unusually high, especially for a semi-arid coniferous forest. Additional measurements of soil CO_2 fluxes were made near this location using a separate measurement system (a LI-COR 6400-9, LI-COR Biosciences) and the magnitudes were equally high. Both methods have been tested in laboratory conditions and can provide robust estimates of soil CO_2 fluxes (Martin et al. 2004, Risk et al. 2011). The large fluxes were unusual and could represent a large signal of root respiration or increased detritus inputs due to the proximity of Chamber 1 to the base of a mature tree (Figure 2). Large spatial

Table 1. Individual bin selection criteria and data ranges for each chamber.

Chamber	Bin	*n*	DOY range	SWC (%)	Soil *T* (°C) at		Ranges (μmol CO_2 m^{-2} s^{-1})	
					2 cm	16 cm	Soil flux	GEP[1]
1	1	18	129–164	>25	4	8	2.01–3.01	0.00–12.65
	2	15	129–164	>25	6	8	2.02–3.13	0.00–14.38
	3	62	205–243	<20	10	14	6.53–15.91	0.00–21.89
	4	50	206–243	<20	12	14	6.61–15.71	0.00–23.41
	5	62	244–262	<20	12	16	5.42–9.25	0.00–16.83
	6	53	244–262	<20	14	16	6.03–8.06	0.00–16.98
2	1	18	129–164	>25	4	8	1.37–1.62	0.00–12.65
	2	15	129–164	>25	6	8	1.43–1.78	0.00–14.38
	3	62	205–243	<20	10	14	3.46–5.20	0.00–21.89
	4	50	206–243	<20	12	14	3.47–5.77	0.00–23.41
	5	62	244–262	<20	12	16	2.75–4.23	0.00–16.83
	6	53	244–262	<20	14	16	2.98–4.05	0.00–16.98
3	1	18	129–164	>25	4	8	0.80–0.97	0.00–12.65
	2	15	129–164	>25	6	8	0.87–1.13	0.00–14.38
	3	62	205–243	<20	10	14	1.96–4.13	0.00–21.89
	4	50	206–243	<20	12	14	1.99–4.17	0.00–23.41
	5	62	244–262	<20	12	16	1.10–2.05	0.00–16.83
	6	53	244–262	<20	14	16	1.09–2.21	0.00–16.98
4	1	18	129–164	>25	4	8	1.08–2.01	0.00–12.65
	2	15	129–164	>25	6	8	1.01–2.32	0.00–14.38
	3	62	205–243	<20	10	14	3.17–5.81	0.00–21.89
	4	50	206–243	<20	12	14	3.10–5.58	0.00–23.41
	5	62	244–262	<20	12	16	2.56–3.38	0.00–16.83
	6	53	244–262	<20	14	16	2.68–3.65	0.00–16.98

DOY, day of year.
[1]Gross ecosystem productivity range represents the range of GEP values at a lag of zero days.

variation of soil CO_2 fluxes in forests is not uncommon (Ohashi and Gyokusen 2007, Ohashi et al. 2007) and 'hot spots' can be very large and persistent (Martin and Bolstad 2009, Søe and Buchmann 2005). Despite the large magnitude of the fluxes, the values do represent real flux conditions and provide a unique opportunity to test the issues associated with diel patterns of soil fluxes as highlighted in the following sections.

Seasonal soil temperature and soil moisture follow predictable trends for the temperate, semi-arid climate (Figure 3b and c). Soil moisture drops considerably each summer during the seasonal dry period, although interannual variation in the duration of each drought event can be large (Thomas et al. 2009). This predictable depletion of soil moisture allowed us to isolate periods where soil moisture limitations would be consistent and not influence the temporal variability of soil fluxes. The deep profile of soil moisture did show moderate temporal variation in deep soil layers when upper soil layers are uniformly dry for extended periods (Figure 3c). This has the potential to influence tree water stress as deeper water sources become limiting. We used an integrated profile soil moisture mean to select uniform conditions discussed in Scenario 3 to avoid this potentially confounding effect on soil CO_2 efflux, which could arise from decreasing deep soil water after shallow soil water conditions had stabilized at the annual minimum.

Diel patterns: spatial and temporal variation

Soil CO_2 flux exhibited strong seasonal variation in the timing of diel cycles, as well as considerable variation in the diel trends among the four chambers (Figure 4, shown as normalized values for each day; values of 1 are maximum daily values and values of 0 are minimum). Early in the season, normalized diel fluxes were similar among all chambers and occurred mid-afternoon, and appeared to coincide with 8 or 16 cm soil temperature peaks (Figure 5). In previous work, these conditions are often assumed to be universal across all seasons. However, our observations show that, as the season progressed, the peak diel flux in Chambers 1–3 occurred progressively later through the dry season until it stabilized as much as 12 h later than the flux peaks that occurred in spring and fall. Midday minimums of soil CO_2 fluxes are not uncommon and have been reported in other dry systems with differential responses between woody vegetation and grasses (Barron-Gafford et al. 2011). The progression of the diel trend in Figure 4 matches well with decreases in soil moisture (Figure 3c), which support the conclusion that either changes in soil porosity or changes in the depth of CO_2 production could cause this pattern

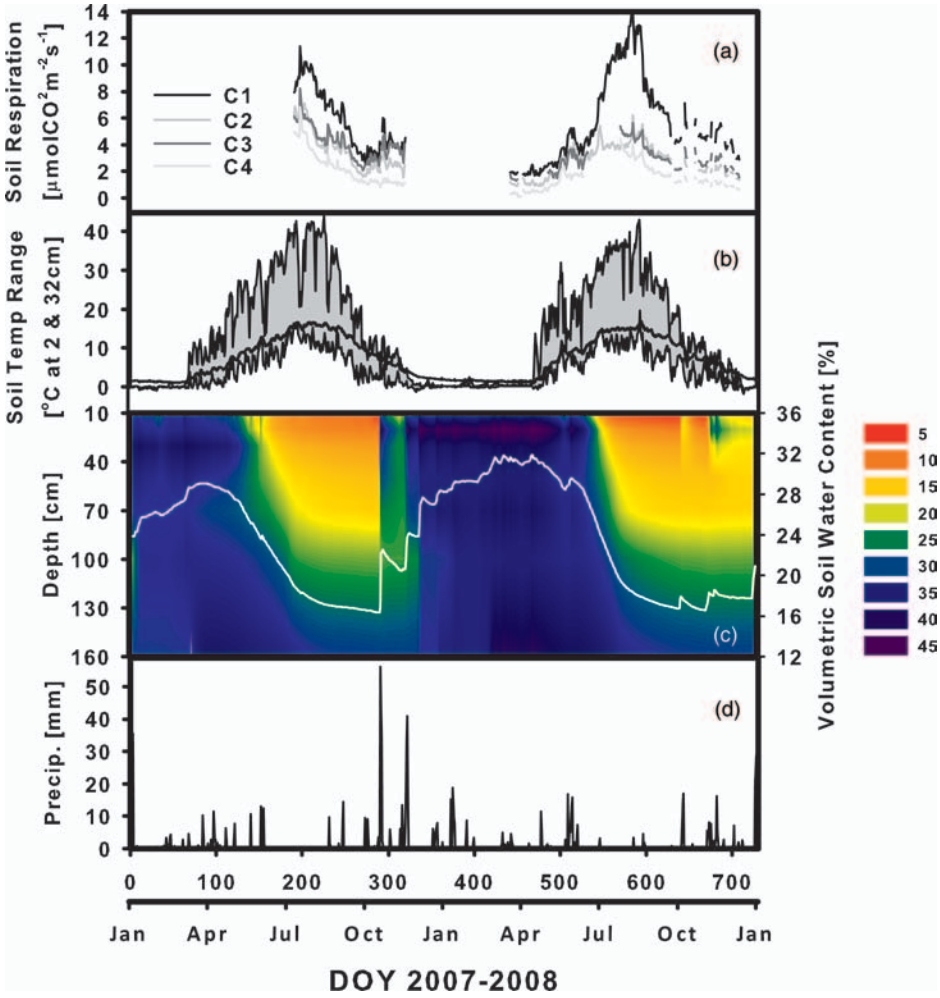

Figure 3. For 2007 and 2008, (a) spatial variation of mean daily soil CO_2 fluxes among the four chambers, (b) large differences in diel soil temperature range at 2 and 32 cm (32 cm range shown in shaded region), (c) deep and consistent decline in summer soil moisture from 10, 20, 30, 50, 70, 100, 130 and 160 cm, which was linearly interpolated between depths with a depth-weighted profile mean shown as a white line, and (d) summed daily precipitation with summer drought conditions clearly visible (July–October).

(Scenarios 1 and 2). However, similar data from a semi-arid system with summer monsoons did not show changes in summer diel trends when the soils were wet (Barron-Gafford et al. 2011), which indicates that allocation/production/phenology of the vegetation nearest the measurements may drive the majority of our pattern.

Observing large variation in magnitudes between sampling locations is common (Martin and Bolstad 2009, Savage et al. 2009); however, spatial variation of diel trends is rarely quantified. This study represents a small survey of the site (~1.25 m^2 of total sample area) but could have been spatially calibrated using large numbers of point measurements as used in Thomas et al. (2009); however, that analysis assumed diel patterns were spatially and temporally consistent. Data from the four chambers examined here indicate that this phenomenon is potentially very important and could strongly influence the generalization of site-level soil CO_2 fluxes and total ecosystem respiration.

Diel patterns: quantifying causes and examining bias-free GEP correlations

Scenario 1: soil water and changing diffusion rates

If the shifting of the diel patterns of soil CO_2 fluxes (Figures 4 and 6a) were caused by observable phenomena, such as a change in the soil CO_2 diffusion coefficient, then models of diffusion rates paired with production at various depths should highlight the magnitude of this issue. Our estimated diffusion coefficients (D_s) varied considerably among seasons (4.5×10^{-6} to 1.8×10^{-5}), largely a function of soil water content. This was expected, as the equation used for estimating diffusion rates is temporally dynamic due to temperature and soil moisture, while all other variables were static. Despite the range of diffusion coefficients, the calculated times needed to diffuse across the various distances (2, 4, 8, 16 and 32 cm) were considerably less than 1 h, except during wet soil conditions when we calculated that it would take ~1.4 h to diffuse a distance of 32 cm. This is

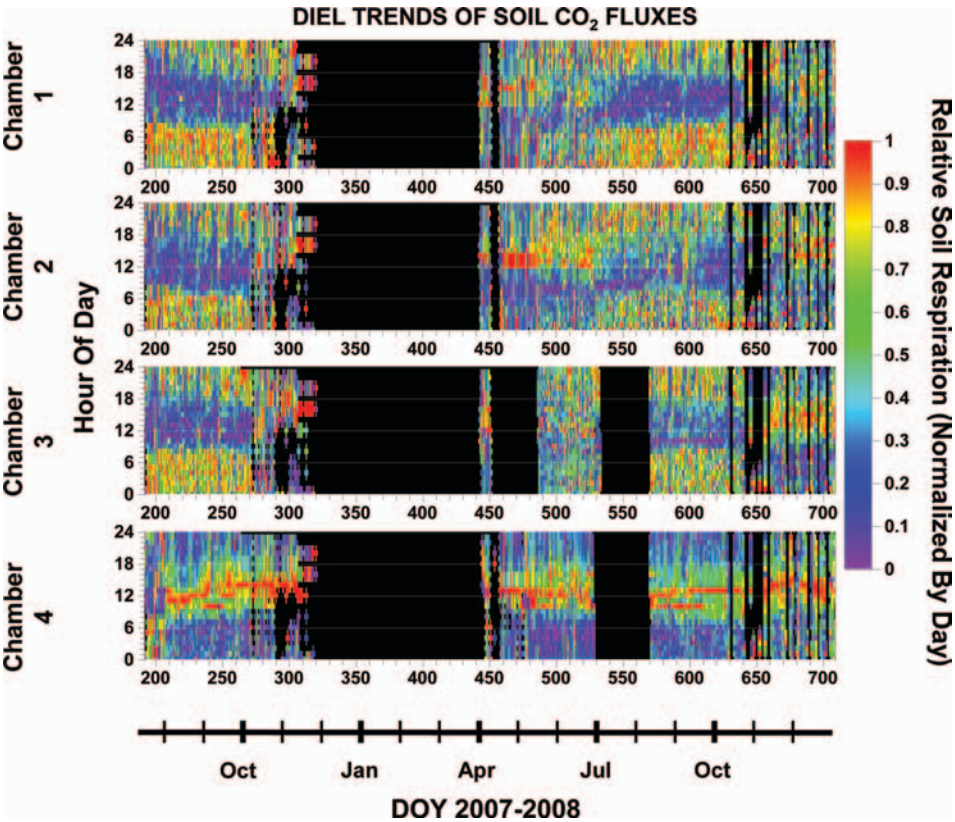

Figure 4. Large seasonal variation of diel soil respiration patterns for each chamber (1–4) over the 2-year period. Hourly soil respiration for each hour was normalized against all values for each day. Each hourly value (*y*-axis) for each day (*x*-axis) is shown as a pixel where a value of 1 (red) denotes the peak respiration for a given day; 0 (purple) is the daily minimum.

similar to the findings of Phillips et al. (2010) where thermal diffusion (the time lags from the propagation of energy through the soil profile) was implicated as being more influential in the diel patterns of soil CO_2 production than gas diffusion lags.

We next used the diffusion rate estimates paired with the peak hour of soil temperature at various depths (Eq. (4)) to predict the time a flux should appear in the chamber. Based on the thermal wave (which started at t_0 at the soil surface), the time of flux varied considerably across seasons and depths (Figure 6b). The predicted values at a given depth were relatively stable for most of the period that included the CO_2 flux measurements, while the observed values of peak fluxes varied from midday to late in the evening or even the following morning (Figure 6b versus a); therefore, it is likely that neither changing diffusion rates nor changing thermal diffusivity would wholly account for the observed shifting of diel patterns. This indicates that the flux could occur at multiple depths across the season, not at a static depth, 4, 8, 16 cm, etc., which is often assumed and used in modeling endeavors. The lack of convincing evidence of diffusion-driven shifts in diel flux patterns does not exclude diffusion as a partial culprit in influencing diel patterns, but our tests show that this effect is small at our sites for snow-free periods.

Scenario 2: a transient CO_2 source

Because variation in both CO_2 diffusion and thermal diffusion rates could not be solely responsible for the seasonality of diel soil CO_2 efflux patterns (Figure 6a and b), we tested whether a shifting CO_2 source at increasingly greater soil depths and the lags caused by thermal diffusion would explain the variation. We found that thermal transfer was linearly related to depth and relatively constant during snow-free periods, as measured by the peak of the diel trend of soil temperature at the various depths (2, 4, 8, 16, 32 and 64 cm); therefore, we assumed that the temperature pulse would propagate down the soil column at a constant rate from the soil surface, represented here by the 2 cm temperature depth. When the temperature pulse reached a given depth, the temperature would instantaneously affect the production of CO_2 and create a pulse of CO_2, bound for the surface and constrained by the diffusion rate (Eq. (1)). The sum of the thermal transfer time and the diffusion time was added to the hour of the initial pulse, which approximated the time of day a flux should appear if it originated from a given depth.

Depth of production estimates were not unreasonable (~30 cm, Figure 6c), and varied by chamber with a trend related to distance from nearest tree (0.6, 1.2, 1.8 and 3.4 m for Chambers 1–4, respectively). This partially supports the argument of a transient dominant source, with the presence of

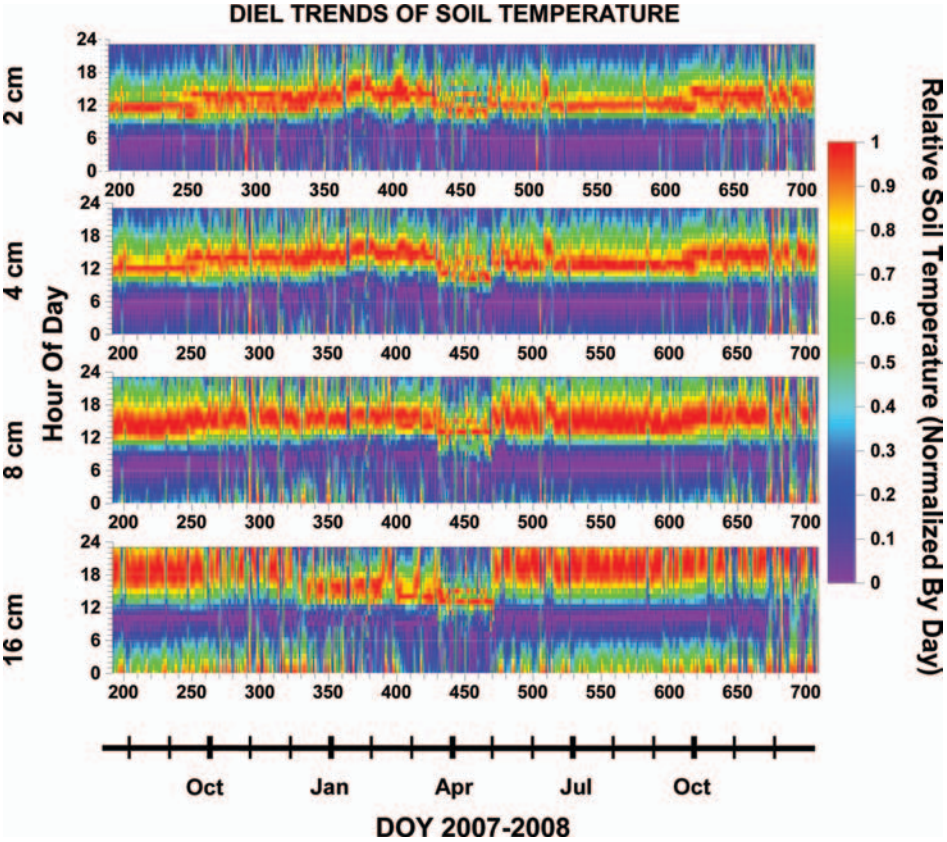

Figure 5. Consistent temporal patterns of diel soil temperature for four depths over the 2-year period. Hourly soil temperature for each hour was normalized against all values for each day. Each hourly value (*y*-axis) for each day (*x*-axis) is shown as a pixel where a value of 1 denotes the peak temperature for a given day at each of four depths (2, 4, 8 and 16 cm); 0 is the daily minimum.

deeper roots nearer the base of trees and shallow roots and shallow shrub roots further from a dominant tree. Furthermore, the hypothesis of a transient CO_2 production source is logical as litter respiration from shallow depths should dominate in spring when soil moisture is high, while deeper sources like root respiration should dominate when the soils are dry. However, during the dry period when our model predicts a production depth of ~30 cm, there was a disproportionally large diel range of soil CO_2 fluxes relative to the small range of temperatures. At a soil depth of 32 cm, the mean diel range of soil temperature was 0.2 °C; therefore, at the corresponding mean range of diel soil CO_2 efflux would result in values of Q_{10} of 8.6×10^4 and as high as 6.1×10^6 if we assume a standard temperature-driven flux. These values of Q_{10} are many orders of magnitude higher than any reported in the literature for any site, at any time, using any method, as well as for any values reported for soil CO_2 fluxes from controlled laboratory experiments (Bahn et al. 2010, Subke and Bahn 2010, Wang et al. 2010), and should therefore be treated as highly suspect and indicative of erroneous causality, i.e., the temperature from that depth cannot be driving the flux.

Likewise, a model of soil flux, based on annual soil moisture and soil temperature data at one of three depths, performed well with low P values and high values for R^2 at the seasonal or annual scale (Eq. (7), Table 2, Figure 6d) but poorly at the hourly scale (Figure 6d, expanded panel) where the difference in timing and magnitude for soil fluxes modeled from various soil temperatures is apparent. The magnitude of modeled fluxes predictably depends on the depth of temperature used in the model, and the magnitude most closely fits observed values when shallow soil temperatures were used (2 cm), while the diel periodicity more closely fits data modeled from between 16 and 32 cm soil temperatures. Unfortunately, at these depths, the magnitude is far less than the observed values. Since the Q_{10} and annual soil respiration model fits indicate that the flux was probably not coming from the predicted depth or the flux was decoupled from temperature, or both, it is possible that we may be lacking the basic understanding of environmental influences in situ on soil CO_2 production and its eventual movement from soil pore space to the atmosphere. It is difficult to understand all of the environmental factors that may drive the diel trends, but it is possible to test the possibility that the fluxes from these dry, stable conditions are decoupled from temperature and potentially coupled to canopy processes (such as GEP).

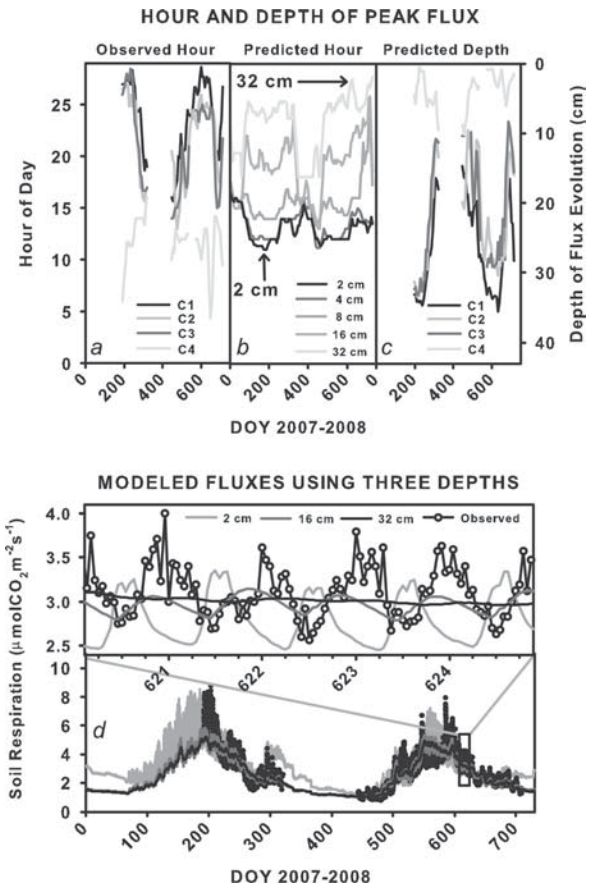

Figure 6. (a) Observed hours of peak diel soil CO_2 flux for Chambers 1–4 do not match the (b) predicted hour of peak diel soil CO_2 flux if a pulse was produced at one of the listed depths, and (c) the theoretical depth of CO_2 production estimated from soil heat transfer and diffusivity models for Chambers 1–4 could range seasonally from ~10 to 30 cm. However, (d) the magnitudes of fluxes within a given day are proportionally much larger than the very small changes in diel soil temperature at 32 cm. *Note*: the 'Hour of Day' axis for (a) and (b) extends beyond 24 h to clarify the progression of peak flux from midday to evening to early morning on the following day; i.e., when peak values were earlier than 0600 PST, 24 h were added to the value.

Scenario 3: robust test for soil CO_2 flux–GEP correlations

Tests of Scenarios 1 and 2 showed that, under traditional paradigms, soil CO_2 flux did not respond to the drivers that have typically been reported to account for the majority of seasonal variation (like soil temperature as used in Martin and Bolstad 2005). It is not without merit that studies have focused on temperature, because temperature does drive a large portion of the variation of decomposition (Gabriel and Kellman 2011). It is also important to note that radiation, vegetative growth/allocation and other seasonal variables mirror seasonal temperature trends; therefore, it is acceptable and most likely correct to assume that temperature may directly or indirectly correlate to the variation at longer scales. However, at smaller time scales (of perhaps a day, an hour or less) when temperature is entwined with other concurrent environmental cycles, it is possible that influences like GEP can mask or even over-ride the temperature response.

To test for GEP effects independently of temperature and moisture, we examined very discrete bins of data of consistent environmental conditions. Because of the large amount of data in the study, we were able to populate a dataset across a large range of GEP conditions at the hourly scale that only includes soil CO_2 flux data from very similar temperature and moisture conditions. The effects of temperature and moisture were minimized by grouping the selective data bins by (i) integrated 0.0–1.6 m soil moisture, (ii) periods free from precipitation that included the previous 5 days and (iii) ±1 °C soil temperature bins at 2 and 16 cm soil depths. Bin selection criteria are listed in Table 1.

At the hourly scale, GEP appeared to be correlated with the soil CO_2 fluxes across the ~20–40 day bins with peak values occurring at multiple lag times across the seasons (Figure 7). During spring (Bins 1 and 2), the correlations exhibited some similarity for Chambers 1–3 with lags at ~10, 21 and 26 days but these lag periods are small. At Chamber 4, the lag peaks

Table 2. Annual soil respiration model parameters and coefficients (Eq. (7)).

	Using soil temperature from		
	2 cm	16 cm	32 cm
Model fit statistics			
R^2	0.616	0.842	0.837
DF_{error}	6689	6689	6689
Model *P* value	<0.0001	<0.0001	<0.0001
Coefficients[1]			
a [intercept]	–5.654670	–2.407183	–2.084905
b [Td]	0.055003	0.118102	0.146020
c [1/SWC]	285.388743	115.009712	98.288787
d [1/SWC × 1/SWC]	–2931.434553	–1138.168238	–1003.436917
e [Td × 1/SWC]	–0.655755	–0.996992	–1.187917
f [YEAR][2]	–0.224454	–0.112640	–0.091804

[1]Coefficients are all significant with *P* values <0.0001.
[2]YEAR refers to a nominal factor when YEAR = 2008; coefficient is 0 when YEAR = 2007.

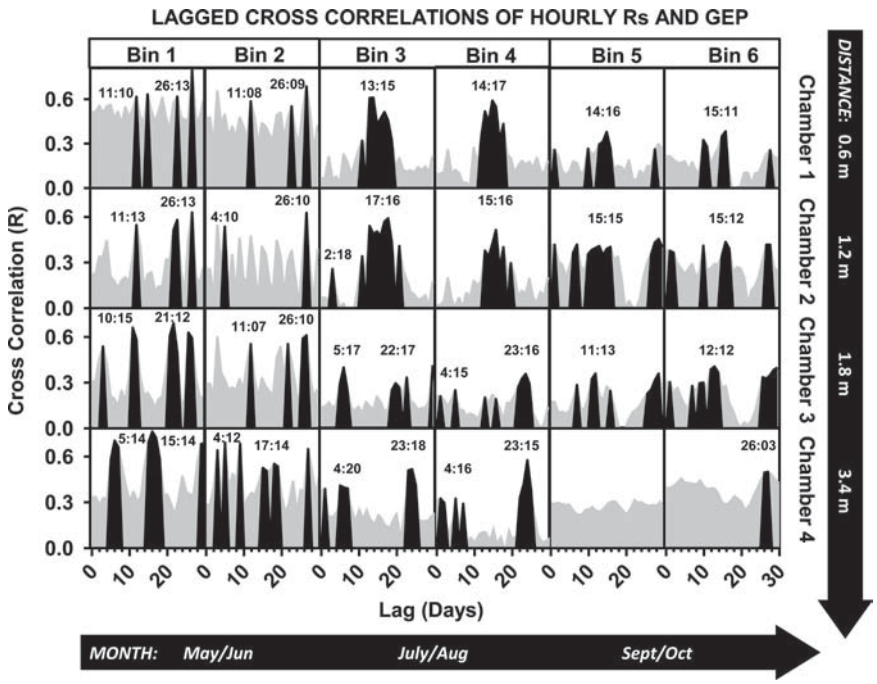

Figure 7. Filtered cross correlations between binned soil CO_2 flux and 6-h running mean of GEP at the hourly scale (black regions, unfiltered data shown in gray) exhibit some consistent periodicity of lags across drought conditions. The lags of notable peaks are labeled with DAY:HOUR. Because GEP is negative, we used $-1 \times$ GEP so that positive correlations shown here represent a positive correlation between photosynthesis and soil CO_2 flux. The bins and chambers are arranged chronologically and spatially with the data from the latest period and from the chamber with the longest path length at the bottom right. Filtered cross correlations consist of only significant relationships with non-zero slopes and trimmed for stationarity (i.e., filtered values must be 50% greater than mean R for all lags). Stationarity of R values was eliminated because a constant R value for all lags reflects non-variable data that are similarly synchronous every 24-h period across all lags. Negative correlations are not shown because they approximately mirror the positive values and were generally not significant.

are more robust with significant values at ~5 and 15 days. The maximum correlations of notable peaks in Figure 7 are marked with the day and hour (in DAY:HOUR format) and highlight the consistency among Chambers 1–3 and across Bins 1 and 2 with relatively consistent lags at 10–11, 21 and 25–26 days. Chamber 4 has repeated lags in Bins 1 and 2 at 4–5 and 15–17 days. Despite the somewhat consistent lags repeated across bins and chambers, caution is needed due to the small range of soil flux data for the conditions of Bins 1 and 2 (Table 1), and because soil moisture and labile carbon, which are both readily available during this period following snow melt, may heighten decomposition and obscure or overshadow any role of canopy processes on soil CO_2 fluxes. Further work should directly address the role of canopy assimilation on soil CO_2 production during periods when decomposition is likely to be high and possibly primed by root-supplied carbohydrates.

As the soils dry in July and August (Bins 3 and 4), peaks of a longer duration are evident. Chamber 4 maintains peaks at ~5 and 23 days but the peaks at 15–17 days are no longer present, possibly due to some change in plant phenology as shallow rooted shrubs go dormant during the drought conditions. At Chambers 1 and 2, a dominant and long-lived peak occurs ~15 days during both bins, while Chamber 3 has multiple smaller peaks, with a dominant peak ~5–7 days later than Chambers 1 and 2. In the autumn (September/October), Chambers 1–3 have similar lags with major peaks again at ~11–15 days.

As the lags change through the seasons, it is possible that we are spanning a range of resolution where GEP effects may be only moderately observable at hourly scales, but other constraints could mask a direct link or create multiple correlations. Additionally, it may be possible that the GEP effect does act at multiple scales (Högberg et al. 2008) despite being buffered by large carbohydrate supplies so that any variation of assimilation only results in small perturbations in C supplied belowground (Vargas et al. 2009). This would be especially apparent in forested systems with large path lengths between leaves and roots (Mencuccini and Hölttä 2010) which can vary non-linearly with tree size (as noted in sap stream CO_2 by Dannoura et al. 2011). Studies such as ours and others may be looking to attribute observed variation to sources that may be relatively stable at hourly and even daily scales. Also, the GEP to soil CO_2 flux pathway may not be direct and may involve many additional unmeasured processes each with separate constraints, thereby creating a diffuse flow and not a direct 'carbon in–carbon out pipeline'. However, recent work has indicated multiple pathways of labeled C as it traveled from the foliage to the atmosphere via the soil (Epron et al.

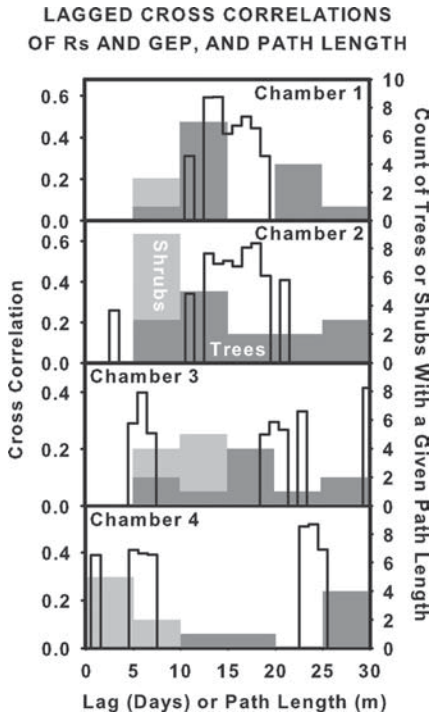

Figure 8. The cross correlations between binned soil CO_2 flux and GEP at the hourly scale (black line) show notable similarity to the distribution of path lengths (distance from chamber + tree height) for all neighboring trees and shrubs within 10 m of each chamber. Light gray bars show the number of shrubs and dark gray shows the number of trees. Shrubs were all <1 m in height so path length is distance from chamber to shrub only. Cross-correlation data are from the fourth set of bin conditions (Table 1, Figure 7).

2011, Heinemeyer et al. 2011). Distinct pathways such as CO_2 from root metabolism and CO_2 from primed microbes, or GEP-modulated root and/or microbial activity or the microbial consumption of tissues that contained labeled C may all have different timing. This could potentially explain the multiple correlations observed here (Figure 7).

Spatial and temporal patterns of soil CO_2 flux–GEP correlations

The correlations between GEP and soil CO_2 fluxes may appear complex (Figure 7), but when viewed across time and space, there appears to be a stronger signal closer to the base of trees and earlier in the dry period (July/August). Although it is compelling that a similar pattern of GEP influence on soil respiration appears at Chambers 1 and 2 across both scales during the summer period, other studies have noted large variation of soil respiration at the sub-meter scale (Martin and Bolstad 2009), so it is not unreasonable to expect large variation in the response of soil fluxes to GEP. A more uniform and definitive lag across all chambers would certainly simplify analyses, but would be unexpected due to the large differences in placement and measurement environment represented by each of the four chambers.

Using the stand survey data (from Figure 2), we compared the chamber-specific lags between GEP and soil CO_2 fluxes with the distribution of path lengths (distance from chamber + tree height) of individual trees within 10 m of each chamber center (Figure 8). Roots may certainly extend beyond 10 m from the base of a tree but the majority of roots should be within this radius. The distribution of these path lengths appears to follow the differences in lagged cross correlations between GEP and soil CO_2 fluxes from each chamber (Figure 8), and may help explain the observed cross-correlation differences across chambers and multiple peaks. Others have reported a strong link between soil fluxes and spatial variation of roots at this scale (Søe and Buchmann 2005, Bréchet et al. 2011, Ceccon et al. 2011) and neighboring tree size can have a measurable impact as well (Katayama et al. 2009, Bréchet et al. 2011).

Scaling and modeling of these processes is currently impractical on such fine spatial scales as examined here, but a site-level correlation between GEP and soil CO_2 flux might be approximated. Using the survey data, we estimated the integrated site-level lag by modeling the spatial distribution of trees and possible lags for a given location. We assumed an even distribution of trees where each tree occupied 30.78 m^2 of ground area. The area was divided into 400 pixels where distance from each pixel to an average tree at the center was added to a mean canopy height of 16.6 m. The distribution of path lengths was positively skewed and had a mode of 19.5 m. Our chambers had dominant path lengths of 10, 10, 15 and 25 m for Chambers 1–4, respectively; therefore, we could assume that a plot-level mean lag between GEP and soil CO_2 flux would be between the lags observed in Chambers 3 and 4, ~20–25 days. This value is purely speculative and tracer studies should be conducted to verify this.

In addition to the variation of path lengths, there was considerable variation in tree/shrub composition surrounding the chambers (Figure 2). This may further complicate attempts to quantify GEP–soil CO_2 flux links if the contributing vegetation has differential diel, seasonal and inter-annual growth patterns as well as rates of C movement from foliage to soil (Carbone and Trumbore 2007). Chamber 4 was 3.4 m away from the nearest tree base but was closely surrounded by shrubs. It may be possible that the large differences in lags between Chambers 1–2 and 3–4 in the spring and summer seasons illustrate the differential influence of tree- or shrub-mediated soil CO_2 production. All chambers are within 1 m of shrubs and show some correlation between soil CO_2 fluxes and GEP lagged 2–5 days (Figure 7). This value would be closer to lags observed using isotopic techniques at very similar sites (Bowling et al. 2002, McDowell et al. 2004), although Bowling et al. (2002) showed an increased correlation as the lag approached their observation limit of 15 days.

Lastly, it appears that many separate lags between GEP and soil CO_2 fluxes dominate in the spring, but are less apparent in

the later season. A seasonal progression of lag times and multiple peaks was seen in microbial C and root respiration of young trees (Epron et al. 2011), and drought has been shown to increase the residence time of C in foliage and decrease the recently assimilated C recovered in soil CO_2 fluxes (Ruehr et al. 2009). Perhaps the patterns seen in Figure 7 illustrate the changing pathways of C as the season progresses and individual trees differentially respond to drought, which could explain the increasing lag times across the year at some of the chamber locations. The late season (September/October) decrease in apparent correlation between soil CO_2 fluxes and GEP may also coincide with a possible decrease in root respiration as allocation patterns shift and root production declines (Andersen et al. 2008).

Our data do show a general, potentially repeatable response between GEP and soil CO_2 fluxes occurring at lags of ~5, 15 and 25 days. The lack of a definitive response complicates efforts to quantify this lag for modeling needs, but provides evidence for the existence of a potentially more complex relationship that is important at the individual measurement scale of 1 m or less. We will not over-speculate as to the nature of the patterns seen in Figures 7 and 8, but we believe it supports the need for additional targeted work that quantifies the spatial variation of soil CO_2 fluxes and the origins of production. Therefore, goals should be shifted to novel experimental techniques that can isolate these individual factors at multiple scales.

Future directions and conclusions

It is our opinion that GEP has a quantifiable role in the production of soil CO_2. However, the nature of this process and the magnitude that it influences soil CO_2 fluxes has and will remain unclear using standard chamber techniques paired with concurrent environmental measurements. It is also possible that there are additional unseen interactions between the positive relationship of assimilation and soil fluxes. A potential negative relationship of sap stream transport of soil CO_2 (Aubrey and Teskey 2009) may exist and, if the magnitude and/or speed of upward flow of sap stream CO_2 during the day is larger than CO_2 production in the soil, it is possible that the soil flux may be reduced through sap stream losses. This is highly speculative and we found no short-term negative correlations between soil fluxes and GEP, so targeted studies are needed. In addition to this unforeseen biological factor affecting soil CO_2 movement, additional physical factors such as wind speed or boundary layer mixing can change diffusion gradients if soil CO_2 concentrations are relatively low and near-surface air CO_2 concentrations are high (Hirsch et al. 2004). Unfortunately, this would most likely reduce the nocturnal flux, which is the opposite effect seen here. Previous work that examined the flow of C from foliage to soil found a similar magnitude and velocity of C transport under both normal and 24-h dark treatments (Kuzyakov and Cheng 2001), thereby indicating a possible circadian rhythm that may not relate directly to assimilation. Also, issues such as diel variation of vertical CO_2 movement through the soil profile (Schneider et al. 2009, Maier et al. 2010), microbial metabolism of exudates (Curiel Yuste et al. 2010) and priming effects on decomposition (Zhu and Cheng 2010) need to be properly resolved before links between soil fluxes and canopy assimilation can be accurately quantified. Complex manipulations and novel approaches are required before high-frequency soil CO_2 fluxes can be fully understood.

Our data show, through the process of elimination, that simple temperature and soil moisture relationships do not consistently explain soil CO_2 fluxes at hourly scales for the semi-arid ponderosa pine stand examined in this study. Other sites may show less extreme seasonal variation in the diel patterns due to finer texture soils, lesser seasonal droughts or other miscellaneous conditions that mute the effects seen here. At these sites, it may also be possible to have very good agreement between soil fluxes and temperatures at one fixed depth, and at a depth that is logical for both production and the diel amplitude of influence on the diel range of fluxes observed; however, we recommend that previous findings be viewed cautiously because the relationship could merely be a coincidental artifact of site conditions. Furthermore, standard soil CO_2 flux models may perform adequately at large scales and can be used to address certain goals, but care needs to be taken when extrapolating data to project processes beyond which there exists a reasonable understanding, such as the fate of soil CO_2 flux under a warmer climate. Lastly, many studies have attempted to quantify the assimilation–soil CO_2 pathway, and meta-analyses such as those by Kuzyakov and Gavrichkova (2010) are invaluable. We echo their assertions that understanding climatically driven decomposition, photosynthate-assisted decomposition and root metabolism are all critical, but other biological and physical factors need to be examined as well.

In summary, we show the following:

(i) Diel cycles of soil fluxes at a semi-arid ponderosa pine forest varied seasonally, with the peak daily flux rates occurring later in the day as soil water content decreased. The high-frequency soil CO_2 flux data were out of phase with instantaneous temperature at various depths, and the lags changed across seasons. Soil conditions (temperature and moisture) cannot be solely responsible for the seasonality of the diel trends or the diel variation.

(ii) Changing soil diffusivity or the depth of soil CO_2 production was most likely not the cause of the temporal discrepancies. Since our data indicate that these distinct diel trends are independent of temperature and other commonly implicated factors, GEP could be a logical driver.

(iii) When the effects of other co-varying factors were removed, a quantifiable relationship between soil CO_2 fluxes and GEP was observable at the chamber scale with lag times seemingly related to the distribution of distances from canopy to soil chamber. This effect was strongest during drought conditions.

Measured hourly soil flux data have tremendous value because of the complexity associated with understanding soil fluxes at hourly time scales and, subsequently, linking these fluxes to discrete events and drivers that similarly occur on an hourly scale. Until we can identify the influential processes and accurately represent them quantitatively, hourly data cannot be robustly simulated and should be measured.

Funding

This work was supported by the Office of Science (BER), U.S. Department of Energy (DOE) (grant DE-FG02-06ER64318), for the AmeriFlux project 'On the effects of disturbance and climate on carbon storage and the exchanges of carbon dioxide, water vapor and energy exchange of evergreen coniferous forests in the Pacific Northwest: integration of eddy flux, plant and soil measurements at a cluster of supersites.'

References

Andersen, C.P., D.L. Phillips, P.T. Rygiewicz and M.J. Storm. 2008. Fine root growth and mortality in different-aged ponderosa pine stands. Can. J. For. Res. 38:1797–1806.

Andrews, J.A., K.G. Harrison, R. Matamala and W.H. Schlesinger. 1999. Separation of root respiration from total soil respiration using carbon-13 labeling during Free-Air Carbon Dioxide Enrichment (FACE). Soil Sci. Soc. Am. J. 63:1429–1435.

Aubrey, D.P. and R.O. Teskey. 2009. Root-derived CO2 efflux via xylem stream rivals soil CO2 efflux. New Phytol. 184:35–40.

Bahn, M., M. Rodeghiero, M. Anderson-Dunn, *et al.* 2008. Soil respiration in European grasslands in relation to climate and assimilate supply. Ecosystems 11:1352–1367.

Bahn, M., I.A. Janssens, M. Reichstein, P. Smith and S.E. Trumbore. 2010. Soil respiration across scales: towards an integration of patterns and processes. New Phytol. 186:292–296.

Barron-Gafford, G.A., R.L. Scott, G.D. Jenerette and T.E. Huxman. 2011. The relative controls of temperature, soil moisture, and plant functional group on soil CO_2 efflux at diel, seasonal, and annual scales. J. Geophys. Res. 116:G01023.

Bolstad, P., K.J. Davis, J. Martin, B.D. Cook and W. Wang. 2004. Component and whole-system respiration fluxes in northern deciduous forests. Tree Physiol. 24:493–504.

Bond-Lamberty, B. and A. Thomson. 2010. Temperature-associated increases in the global soil respiration record. Nature 464:579–582.

Bond-Lamberty, B., C. Wang and S.T. Gower. 2005. Spatiotemporal measurement and modeling of stand-level boreal forest soil temperatures. Agric. For. Meteorol. 131:27–40.

Bowling, D.R., N.G. McDowell, B.J. Bond, B.E. Law and J.R. Ehleringer. 2002. ^{13}C content of ecosystem respiration is linked to precipitation and vapor pressure deficit. Oecologia 131:113–124.

Bréchet, L., S. Ponton, T. Alméras, D. Bonal and D. Epron. 2011. Does spatial distribution of tree size account for spatial variation in soil respiration in a tropical forest? Plant Soil 347:293–303.

Carbone, M.S. and S.E. Trumbore. 2007. Contribution of new photosynthetic assimilates to respiration by perennial grasses and shrubs: residence times and allocation patterns. New Phytol. 176:124–135.

Carbone, M.S., G.C. Winston and S.E. Trumbore. 2008. Soil respiration in perennial grass and shrub ecosystems: linking environmental controls with plant and microbial sources on seasonal and diel timescales. J. Geophys. Res. Biogeosci. 113:G02022.

Ceccon, C., P. Panzacchi, F. Scandellari, L. Prandi, M. Ventura, B. Russo, P. Millard and M. Tagliavini. 2011. Spatial and temporal effects of soil temperature and moisture and the relation to fine root density on root and soil respiration in a mature apple orchard. Plant Soil 342:195–206.

Chapin, F.S.I., J. McFarland, D.A. McGuire, E.S. Euskirchen, R.W. Ruess and K. Kielland. 2009. The changing global carbon cycle: linking plant–soil carbon dynamics to global consequences. J. Ecol. 97:840–850.

Curiel Yuste, J., S. Ma and D. Baldocchi. 2010. Plant-soil interactions and acclimation to temperature of microbial-mediated soil respiration may affect predictions of soil CO_2 efflux. Biogeochemistry 98:127–138.

Dannoura, M., P. Maillard, C. Fresneau, C. Plain, D. Berveiller, D. Gerant, C. Chipeaux, A. Bosc, J. Ngao, C. Damesin, D. Loustau and D. Epron. 2011. In situ assessment of the velocity of carbon transfer by tracing ^{13}C in trunk CO_2 efflux after pulse labelling: variations among tree species and seasons. New Phytol. 190:181–192

De Deyn, G.B., H. Quirk, S. Oakley, N. Ostle and R.D. Bardgett. 2011. Rapid transfer of photosynthetic carbon through the plant-soil system in differently managed species-rich grasslands. Biogeosciences 8:1131–1139.

Epron, D., J. Ngao, M. Dannoura, *et al.* 2011. Seasonal variations of belowground carbon transfer assessed by in situ $^{13}CO_2$ pulse labelling of trees. Biogeosci. Discuss. 8:885–919.

Fang, C. and J.B. Moncrieff. 2001. The dependance of coil CO_2 efflux on temperature. Soil Biol. Biochem. 22:155–165.

Gabriel, C.E. and L. Kellman. 2011. Examining moisture and temperature sensitivity of soil organic matter decomposition in a temperate coniferous forest soil. Biogeosci. Discuss. 8:1369–1409.

Graf, A., L. Weihermüller, J.A. Huisman, M. Herbst, J. Bauer and H. Vereecken. 2008. Measurement depth effects on the apparent temperature sensitivity of soil respiration in field studies. Biogeosciences 5:1175–1188.

Heimann, M. and M. Reichstein. 2008. Terrestrial ecosystem carbon dynamics and climate feedbacks. Nature 451:289–292.

Heinemeyer, A., M. Wilkinson, R. Vargas, J.A. Subke, E. Casella, J.I.L. Morison and P. Ineson. 2011. Exploring the 'overflow tap' theory: linking forest soil CO_2 fluxes and individual mycorrhizosphere components to photosynthesis. Biogeosci. Discuss. 8:3155–3201.

Heitjans, P. and J. Kärger. 2005. Diffusion in condensed matter: methods, materials, models. Springer-Verlag, Berlin, p 965.

Hirsch, A.I., S.E. Trumbore and M.L. Goulden. 2004. The surface CO_2 gradient and pore-space storage flux in a high-porosity litter layer. Tellus B 56:312–321.

Högberg, P., M.N. Högberg, S.G. Göttlicher, *et al.* 2008. High temporal resolution tracing of photosynthate carbon from the tree canopy to forest soil microorganisms. New Phytol. 177:220–228.

Högberg, P., S. Bhupinderpal, M.O. Löfvenius and A. Nordgren. 2009. Partitioning of soil respiration into its autotrophic and heterotrophic components by means of tree-girdling in old boreal spruce forest. For. Ecol. Manag. 257:1764–1767.

Horwath, W.R., K.S. Pregitzer and E.A. Paul. 1994. ^{14}C Allocation in tree-soil systems. Tree Physiol. 14:1163–1176.

Irvine, J., B.E. Law and M.R. Kurpius. 2005. Coupling of canopy gas exchange with root and rhizosphere respiration in a semi-arid forest. Biogeochemistry 73:271–282.

Irvine, J., B.E. Law, J.G. Martin and D. Vickers. 2008. Interannual variation in soil CO_2 efflux and the response of root respiration to climate and canopy gas exchange in mature ponderosa pine. Glob. Change Biol. 14:2848–2859.

Janssens, I.A., A.S. Kowalski and R. Ceulemans. 2001. Forest floor CO_2 fluxes estimated by eddy covariance and chamber-based model. Agric. For. Meteorol. 106:61–69.

Katayama, A., T. Kume, H. Komatsu, M. Ohashi, M. Nakagawa, M. Yamashita, K. Otsuki, M. Suzuki and Kumagai TO. 2009. Effect of forest structure on the spatial variation in soil respiration in a Bornean tropical rainforest. Agric. For. Meteorol. 149:1666–1673.

Kuzyakov, Y. and O. Gavrichkova. 2010. REVIEW: Time lag between photosynthesis and carbon dioxide efflux from soil: a review of mechanisms and controls. Glob. Change Biol. 16:3386–3406.

Kuzyakov, Y. and W. Cheng. 2001. Photosynthesis controls of rhizosphere respiration and organic matter decomposition. Soil Biol. Biochem. 33:1915–1925.

Law, B.E., M.G. Ryan and P.M. Anthoni. 1999. Seasonal and annual respiration of a ponderosa pine ecosystem. Glob. Change Biol. 5:169–182.

Lloyd, J. and J.A. Taylor. 1994. On the temperature dependence of soil respiration. Funct. Ecol. 8:315–323.

Maier, M., H. Schack-Kirchner, E.E. Hildebrand and J. Holst. 2010. Pore-space CO2 dynamics in a deep, well-aerated soil. Eur. J. Soil Sci. 61:877–887.

Maljanen, M., P.J. Martikainen, H. Aaltonen and J. Silvola. 2002. Short-term variation in fluxes of carbon dioxide, nitrous oxide and methane in cultivated and forested organic boreal soils. Soil Biol. Biochem. 34:577–584.

Martin, J.G. and P.V. Bolstad. 2005. Annual soil respiration in broadleaf forests of northern Wisconsin: influence of moisture and site biological, chemical, and physical characteristics. Biogeochemistry 73:149–182.

Martin, J.G. and P.V. Bolstad. 2009. Variation of soil respiration at three spatial scales: components within measurements, intra-site variation and patterns on the landscape. Soil Biol. Biochem. 41:530–543.

Martin, J.G., P.V. Bolstad and J.M. Norman. 2004. A carbon dioxide flux generator for testing infrared gas analyzer-based soil respiration systems. Soil Sci. Soc. Am. J. 68:514–518.

McDowell, N.G., D.R. Bowling, B.J. Bond, J. Irvine, B.E. Law, P. Anthoni and J.R. Ehleringer. 2004. Response of the carbon isotopic content of ecosystem, leaf, and soil respiration to meteorological and physiological driving factors in a *Pinus ponderosa* ecosystem. Glob. Biogeochem. Cy. 18:GB1013.

Mencuccini, M. and T. Hölttä. 2010. The significance of phloem transport for the speed with which canopy photosynthesis and belowground respiration are linked. New Phytol. 185:189–203.

Mitchell, S., K. Beven, J. Freer and B. Law. 2011. Processes influencing model-data mismatch in drought-stressed, fire-disturbed eddy flux sites. J. Geophys. Res. 116:G02008.

Moldrup, P., T. Olesen, T. Komatsu, S. Yoshikawa, P. Schjønning and D.E. Rolston. 2003. Modeling diffusion and reaction in soils: X. A unifying model for solute and gas diffusivity in unsaturated soil. Soil Sci. 168:321–337.

Ohashi, M. and K. Gyokusen. 2007. Temporal change in spatial variability of soil respiration on a slope of Japanese cedar (*Cryptomeria japonica* D. Don) forest. Soil Biol. Biochem. 39:1130–1138.

Ohashi, M., T. Kume, S. Yamane and M. Suzuki. 2007. Hot spots of soil respiration in an Asian tropical rainforest. Geophys. Res. Lett. 34:L08705.

Pendall, E., S. Bridgham, P.J. Hanson, *et al.* 2004. Below-ground process responses to elevated CO_2 and temperature: a discussion of observations, measurement methods, and models. New Phytol. 162:311–322.

Phillips, C.L., N. Nickerson, D. Risk and B.J. Bond. 2010. Interpreting diel hysteresis between soil respiration and temperature. Glob. Change Biol. 17:515–527.

Raich, J.W. and W.H. Schlesinger. 1992. The global carbon dioxide flux in soil respiration and its relationship to vegetation and climate. Tellus B 44:81–99.

Risk, D., N. Nickerson, C. Creelman, G. McArthur and J. Owens. 2011. Forced diffusion soil flux: a new technique for continuous monitoring of soil gas efflux. Agric. For. Meteorol. 151:1622–1631.

Riveros-Iregui, D.A., R.E. Emanuel, D.J. Muth, B.L. McGlynn, H.E. Epstein, D.L. Welsch, V.J. Pacific and J.M. Wraith. 2007. Diurnal hysteresis between soil CO_2 and soil temperature is controlled by soil water content. Geophys. Res. Lett. 34:L17404.

Riveros-Iregui, D.A., B.L. McGlynn, H.E. Epstein and D.L. Welsch. 2008. Interpretation and evaluation of combined measurement techniques for soil CO_2 efflux: discrete surface chambers and continuous soil CO2 concentration probes. J. Geophys. Res. 113:G04027.

Rolston, D.E. and P. Moldrup. 2002. Gas diffusivity. *In* Methods of Soil Analysis: Part 4—Physical Methods. Eds. J.H. Dane and G.C. Topp. Soil Science Society of America, Madison, WI, pp 1113–1139.

Ruehr, N.K. and N. Buchmann. 2010. Soil respiration fluxes in a temperate mixed forest: seasonality and temperature sensitivities differ among microbial and root-rhizosphere respiration. Tree Physiol. 30:165–176.

Ruehr, N.K., C.A. Offermann, A. Gessler, J.B. Winkler, J.P. Ferrio, N. Buchmann and R.L. Barnard. 2009. Drought effects on allocation of recent carbon: from beech leaves to soil CO_2 efflux. New Phytol. 184:950–961.

Ruehr, N.K., A. Knohl and N. Buchmann. 2010. Environmental variables controlling soil respiration on diurnal, seasonal and annual timescales in a mixed mountain forest in Switzerland. Biogeochemistry 98:153–170.

Ryan, M.G. and B.E. Law. 2005. Interpreting, measuring, and modeling soil respiration. Biogeochemistry 73:3–27.

Savage, K., E.A. Davidson, A.D. Richardson and D.Y. Hollinger. 2009. Three scales of temporal resolution from automated soil respiration measurements. Agric. For. Meteorol. 149:2012–2021.

Schlesinger, WH. 1977. Carbon balance in terrestrial detritus. Annu. Rev. Ecol. Syst. 8:51–81.

Schneider, J., L. Kutzbach, S. Schulz and M. Wilmking. 2009. Overestimation of CO_2 respiration fluxes by the closed chamber method in low-turbulence nighttime conditions. J. Geophys. Res. 114:G03005.

Sierra, C.A., M.E. Harmon, E. Thomann, S.S. Perakis and H.W. Loescher. 2010. Amplification and dampening of soil respiration by changes in temperature variability. Biogeosci. Discuss. 7:8979–9008.

Sitch, S., C. Huntingford, N. Gedney, *et al.* 2008. Evaluation of the terrestrial carbon cycle, future plant geography and climate-carbon cycle feedbacks using five Dynamic Global Vegetation Models (DGVMs). Glob. Change Biol. 14:2015–2039.

Søe, A.R.B. and N. Buchmann. 2005. Spatial and temporal variations in soil respiration in relation to stand structure and soil parameters in an unmanaged beech forest. Tree Physiol. 25:1427–1436.

Subke, J-A and M. Bahn. 2010. On the 'temperature sensitivity' of soil respiration: can we use the immeasurable to predict the unknown? Soil Biol. Biochem. 42:1653–1656.

Subke, J.A., N.R. Voke, V. Leronni, M.H. Garnett and P. Ineson. 2010. Dynamics and pathways of autotrophic and heterotrophic soil CO_2 efflux revealed by forest girdling. J. Ecol. 99:186–193.

Thomas, C.K., B.E. Law, J. Irvine, J.G. Martin, J.C. Pettijohn and K.J. Davis. 2009. Seasonal hydrology explains interannual and seasonal variation in carbon and water exchange in a semiarid mature ponderosa pine forest in central Oregon. J. Geophys. Res. Biogeosci. 114:G04006.

Vargas, R., S.E. Trumbore and M.F. Allen. 2009. Evidence of old carbon used to grow new fine roots in a tropical forest. New Phytol. 182:710–718.

Vargas, R., D.D. Baldocchi, M. Bahn, P.J. Hanson, K.P. Hosman, L. Kulmala, J. Pumpanen and B. Yang. 2011. On the multi-temporal correlation between photosynthesis and soil CO_2 efflux: reconciling lags and observations. New Phytol. 191:1006–1017.

Vickers, D., C.K. Thomas, J. Irvine, C. Pettijohn, J.G. Martin and B.E. Law. 2012. Five years of carbon fluxes and inherent water-use efficiency at two semi-arid pine forests with different disturbance histories. Tellus B Chem. Phys. Meteorol. (in press).

Wang, X., S. Piao, P. Ciais, I.A. Janssens, M. Reichstein, S. Peng and T. Wang. 2010. Are ecological gradients in seasonal Q_{10} of soil respiration explained by climate or by vegetation seasonality? Soil Biol. Biochem. 42:1728–1734.

Zhu, B. and W. Cheng. 2010. Rhizosphere priming effect increases the temperature sensitivity of soil organic matter decomposition. Glob. Change Biol. 17:2172–2183.